

*Citation for published version:*

Wang, W, Spaven, F, Zhang, M, Baghdadi, M & Coombs, T 2014, 'Direct measurement of the vortex migration caused by traveling magnetic wave', *Applied Physics Letters*, vol. 104, no. 3, pp. 032602.  
<https://doi.org/10.1063/1.4862788>

*DOI:*

[10.1063/1.4862788](https://doi.org/10.1063/1.4862788)

*Publication date:*

2014

*Document Version*

Early version, also known as pre-print

[Link to publication](#)

## University of Bath

### Alternative formats

If you require this document in an alternative format, please contact:  
[openaccess@bath.ac.uk](mailto:openaccess@bath.ac.uk)

#### General rights

Copyright and moral rights for the publications made accessible in the public portal are retained by the authors and/or other copyright owners and it is a condition of accessing publications that users recognise and abide by the legal requirements associated with these rights.

#### Take down policy

If you believe that this document breaches copyright please contact us providing details, and we will remove access to the work immediately and investigate your claim.

## Direct measurement of the vortex migration caused by traveling magnetic wave

Wei Wang, Fred Spaven, Min Zhang, Mehdi Baghdadi, and Timothy Coombs

Citation: [Applied Physics Letters](#) **104**, 032602 (2014); doi: 10.1063/1.4862788

View online: <http://dx.doi.org/10.1063/1.4862788>

View Table of Contents: <http://scitation.aip.org/content/aip/journal/apl/104/3?ver=pdfcov>

Published by the [AIP Publishing](#)

---

### Articles you may be interested in

Stray field enhanced vortex dissipation in YBa<sub>2</sub>Cu<sub>3</sub>O<sub>7</sub>/La<sub>0.7</sub>Sr<sub>0.3</sub>MnO<sub>3</sub>/YBa<sub>2</sub>Cu<sub>3</sub>O<sub>7</sub> hetero-epitaxial tri-layer  
*Appl. Phys. Lett.* **103**, 012601 (2013); 10.1063/1.4813110

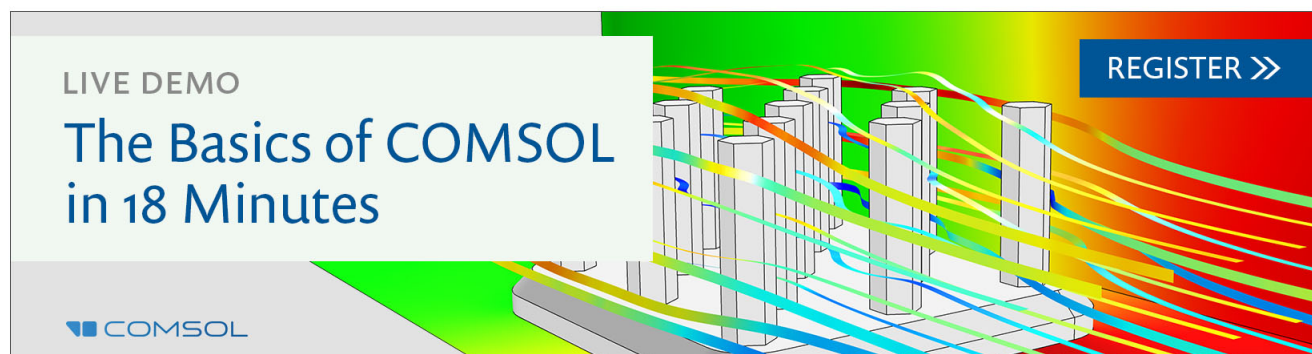
Vortex migration caused by travelling magnetic wave in a 2 in. diameter YBa<sub>2</sub>Cu<sub>3</sub>O<sub>7</sub>- $\delta$  thin film  
*J. Appl. Phys.* **113**, 213906 (2013); 10.1063/1.4809479

Control of the vortex movement and arrangement by out-of-plane magnetic structures in twinned YBa<sub>2</sub>Cu<sub>3</sub>O<sub>7</sub>- $\delta$ /La<sub>0.67</sub>Sr<sub>0.33</sub>MnO<sub>3</sub> bilayer  
*Appl. Phys. Lett.* **86**, 152501 (2005); 10.1063/1.1900307

Microwave impedance of YBa<sub>2</sub>Cu<sub>3</sub>O<sub>7</sub>- $\delta$  high-temperature superconductor films in a magnetic field  
*Low Temp. Phys.* **31**, 254 (2005); 10.1063/1.1884427

Quasiparticle properties of d-wave superconductors in the vortex state  
*AIP Conf. Proc.* **483**, 341 (1999); 10.1063/1.59600

---

A promotional banner for COMSOL. On the left, a white box contains the text 'LIVE DEMO' and 'The Basics of COMSOL in 18 Minutes'. Below this is the COMSOL logo. The background of the banner features a 3D model of a multi-layered structure with colorful, flowing lines representing magnetic field lines or vortices. In the top right corner, there is a blue button with the text 'REGISTER >>'.

# Direct measurement of the vortex migration caused by traveling magnetic wave

Wei Wang (王为),<sup>a)</sup> Fred Spaven, Min Zhang, Mehdi Baghdadi, and Timothy Coombs  
 Electric Engineering Division, Department of Engineering, University of Cambridge, Cambridge,  
 United Kingdom

(Received 6 June 2013; accepted 19 November 2013; published online 21 January 2014)

We studied the magnetisation of a 2 in. diameter YBCO thin film in the presence of traveling magnetic waves with six hall sensors. Simulation based on finite element method was conducted to reproduce the process of magnetisation. We discovered that the magnetisation of YBCO thin film based on traveling waves does not follow the constant current density assumption as used in the standing wave condition. We have shown that the traveling wave is more efficient in transporting the flux into the YBCO thin film, which suggests the potential of a flux injection device for high temperature superconducting coils. © 2014 AIP Publishing LLC. [<http://dx.doi.org/10.1063/1.4862788>]

Magnetisation of type-II superconductors has been studied over decades. It was generally accepted that the magnetisation is due to the pinning of vortices which penetrated into the type-II superconductors. The pinning force shapes the flux line lattice into magnetic gradient which ends up with circulating current according to Ampere's law. The pinning force is a function of thermal fluctuation and grain direction for anisotropic structures, while the inter-vortex forces are a function of density, spin direction, geometry, etc. In general, the constitutive relation in a type-II superconductor can be very complicated, which depends on the temperature, field density, field direction, etc. However, the most intuitive understanding of the problem can be obtained by simply assuming the constant critical current  $J_C$  inside the type-II superconductor, i.e., the Bean's critical state model.<sup>1</sup> To date, Bean model remains a very powerful tool to understand the general magnetisation problem in type-II superconductors. The constant critical magnetic gradient appears frequently in text books on the electromagnetism of type-II superconductor.<sup>2</sup>

Brandt had theoretically shown that type-II superconducting cylinders with different demagnetization factors may end up with different magnetisation profile.<sup>3</sup> His study was based on the standard standing wave condition, i.e., uniform background field. In our study, we would like to show that, for type-II superconductors of large demagnetization factor, the application of a traveling wave may end up with an even more unexpected magnetisation profile. This work is the follow up of our previous publication<sup>4</sup> which suggested that the traveling wave causes local vortex migration, which is very different from the standing wave condition. To date, most theoretical studies for the ac losses were based on the standing wave, however, ac losses is more common in traveling wave conditions such as inside a superconducting motor. This work tries to provide experimental evidence to show that the traveling wave can result in a rather different magnetisation profile in a YBCO thin film.

This work also attempts to explain the emerging flux pump technique for high temperature superconducting (HTS) coils from the viewpoint of vortex migration. Bai and Hoffman had reported the successful magnetisation of a YBCO coil to its critical current with either a linear three phase winding<sup>5</sup> or a rotating magnet.<sup>6</sup> Recently, Walsh had reported the magnetization of a 2 T NMR relaxometry magnet with a rotating magnet.<sup>7</sup> Although the operations of these reported devices are quite successful, the underlying physics is not clearly understood.

The apparatus we used to study this problem is called the circular-type magnetic flux pump (CTMFP) device.<sup>8</sup> This device can produce an annular shape traveling wave which fits our round YBCO sample. The experimental setup and some early experimental results of the CTMFP system had been reported in our previous publications.<sup>4,8,9</sup> The CTMFP is the conceptual combination of the thermally actuated flux pump<sup>10</sup> and the linear type magnetic flux pump (LTMFP).<sup>11</sup> Fig. 1(a) shows the core components of the CTMFP device. It comprises two CTMFP magnets, with each magnet containing a three phasing winding and a dc coil. The purpose of two identical CTMFP magnets is to eliminate the influence of cross field<sup>12</sup> or flux shaking effect<sup>13</sup> in the centre of the gap. The sample is a 2 in. diameter YBCO thin film provided by Ceraco Ceramic Coating GmbH, Germany. The YBCO layer is 200 nm thick and is deposited on  $\text{Al}_2\text{O}_3$  wafer. Six Hall sensors are placed along a radius of the device as shown in Figs. 1(a) and 1(b). The Hall sensors are arranged 5 mm apart. The six hall sensors are connected to a multi-channel data acquisition card Agilent U2353A. The real-time Hall voltages are collected and calibrated by a Labview program. In order to determine the phase of the traveling wave, another Hall sensor is attached in the back of the CTMFP coil as shown in Fig. 1(a).

The numerical simulation is based on the H-formulation.<sup>14</sup> The governing equation is the combination of Faraday's law and Ampere's law, which is solved by the finite element (FEM) software. The governing equation is rearranged as<sup>15</sup>

$$\mu_r \mu_0 \frac{\partial \mathbf{H}}{\partial t} + \nabla \times (\rho \nabla \times \mathbf{H}) = 0. \quad (1)$$

<sup>a)</sup>Email: ww283@cam.ac.uk. Tel.: 0044 (0)1223 748324. FAX: 0044 (0) 1223 332662/748348

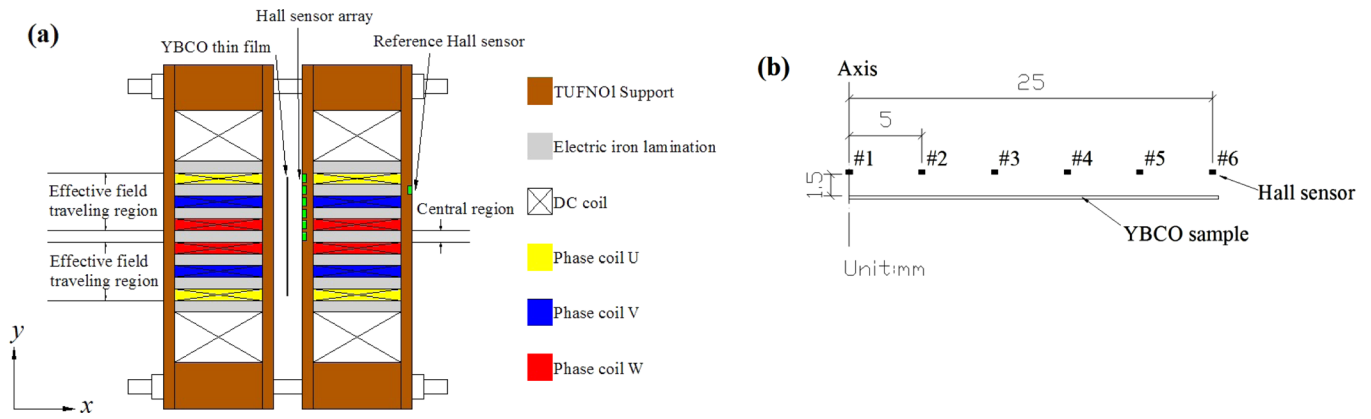
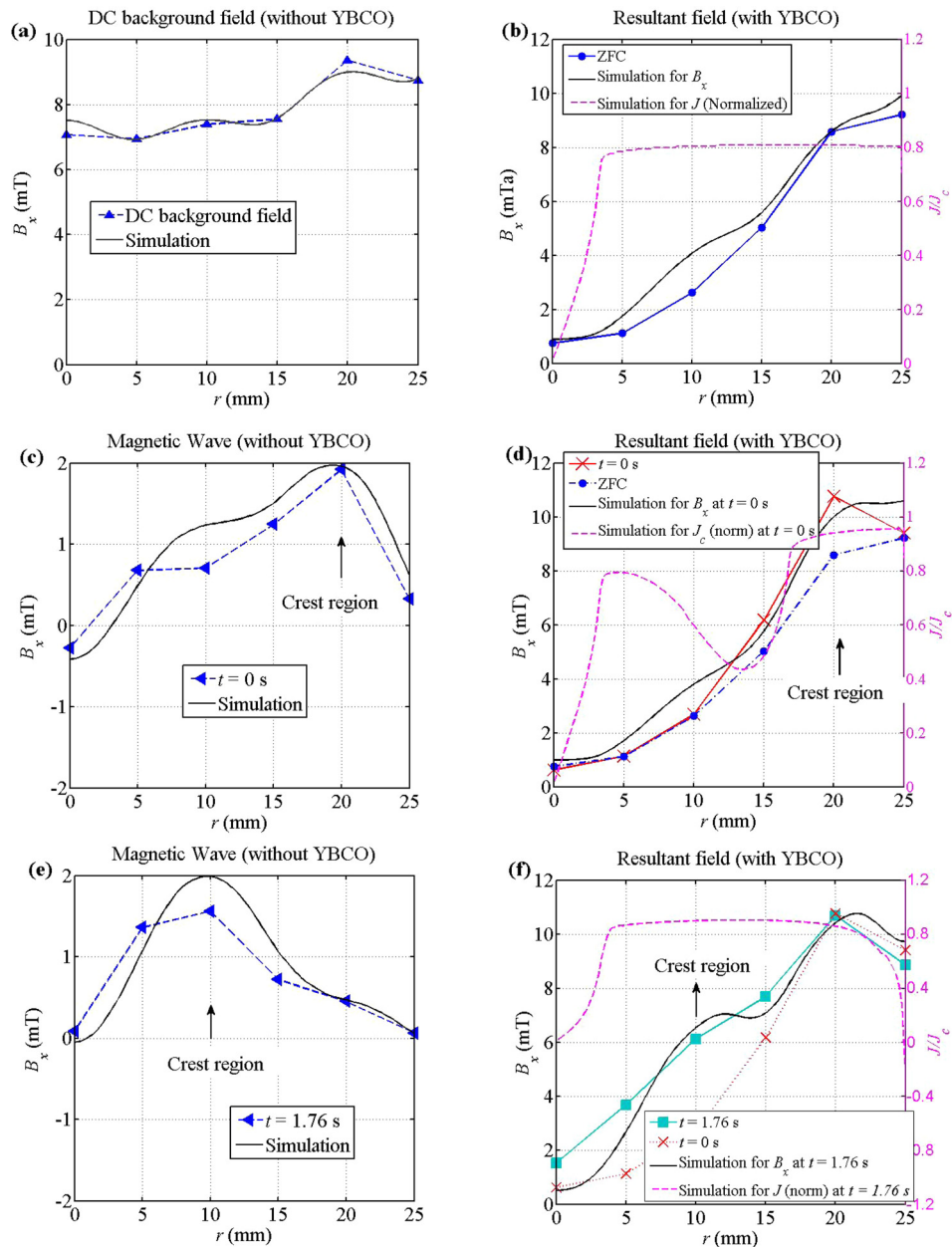


FIG. 1. The circular-type magnetic flux pump device. (a) The CTMFP; (b) the six hall sensor array.

FIG. 2. The measured evolution of the magnetic gradient and calculated current density distributions (normalized by  $J_c$ ) after applied the traveling magnetic wave. The left column shows the measured field (dc background field and traveling wave) without the YBCO sample, while the right column shows the resultant field with the YBCO sample.

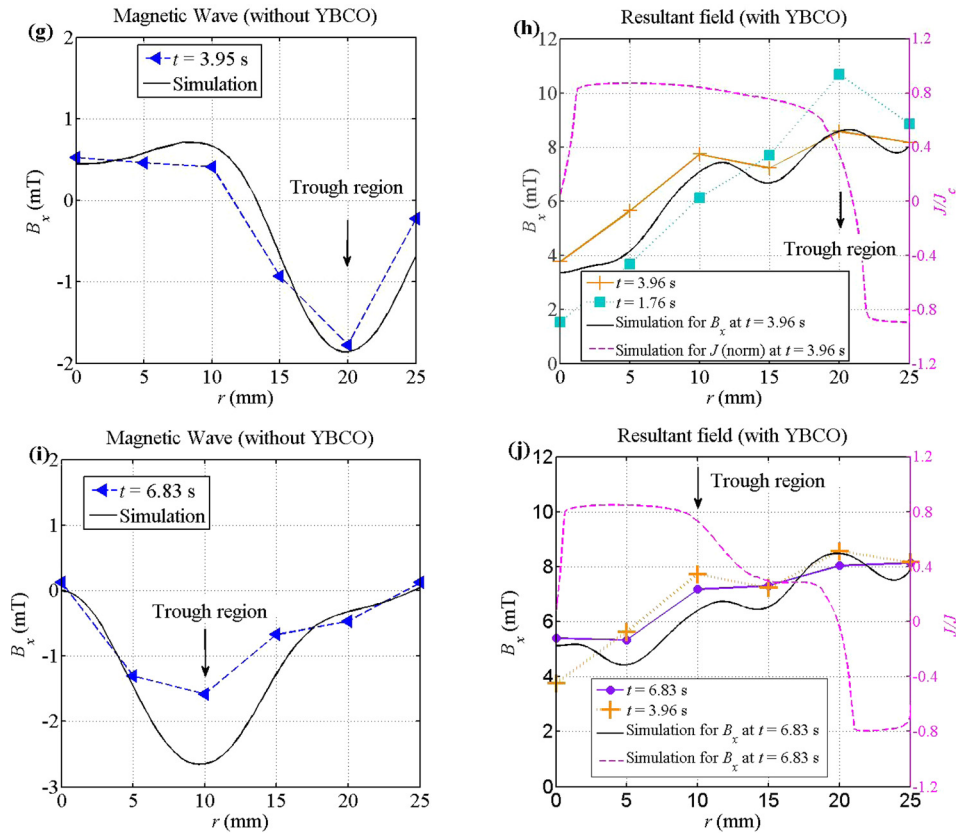


FIG. 2. (Continued)

In the axial symmetric model, two components of the magnetic field were solved:  $\mathbf{H} = [H_r, H_z]^T$ . For the YBCO sample,  $\rho$  is derived from the E-J power law, which is expressed as:  $\rho = J^{n-1} E_C / J_c^n$ . We use  $J_c = 1.87$  MA/cm<sup>2</sup>,  $n = 30$ , and  $E_C = 10^{-4}$  V/m in our calculation. The values of  $J_c$  and  $n$  are derived by fitting the simulation with the logarithmic decay curve<sup>16</sup> obtained from the magnetisation measurement. The anisotropy and the field dependency of the critical current are not considered in the calculation, since the applied field is always normal to the sample surface and the applied traveling wave varies in a small range ( $\sim 2.0$  mT).

We have shown in our previous publication<sup>4</sup> that the traveling wave can help the vortex to migration into the centre of the YBCO sample after the zero-field cooling (ZFC). In this experiment, we perform this experiment again with six hall sensor array. The output voltage of the inverter is increased to 10 V and the amplitude of the traveling wave is about 2 mT. The frequency is set as 0.1 Hz. We are interested in why the field in the centre increases drastically and how the current inside the superconductor changes due to the traveling wave. In Fig. 2, we show the process as the field in the centre rises up as the wave travels. Simulation results are also shown in these figures to show the validity of the model. The calculated current density distributions are plotted in the figures as well to help understand the magnetisation process.

The left column in Fig. 2 shows the applied field without a superconductor, i.e., dc background field in Fig. 2(a) and the traveling magnetic wave in Figs. 2(c)–2(i), while the dc background field (Fig. 2(a)) was present in the whole

experimental process. The right column in Fig. 2 shows the measured field in the presence of the YBCO sample at corresponding time: Fig. 2(b) shows the magnetic shielding profile after applying the dc background field; Figs. 2(d)–2(j) show the resultant field at corresponding phase of the applied traveling wave as shown in the left column. We have also plotted the calculated current density profiles in each time step. Since the sample is very thin (200 nm), the current density does not change across the thickness as can be verified from the model. Therefore, we take the current density across the centre of the sample, then normalized by its critical current  $J_c$ .

In Fig. 2(b), as the standing wave is applied to the sample, there is clearly a magnetic shielding profile. The simulation shows that the current is constant across the radius and is about 80% of  $J_c$ . This is a very typical magnetisation profile after applying a standing wave as suggested by Bean model.<sup>1</sup> In Figs. 2(c) and 2(d), as the crest region of the traveling wave arrives at  $r = 20$  mm, the current density near the edge of the sample increases to about 95% of  $J_c$ , while the current density in the inner area drops to 45% of  $J_c$ . As the crest region travels further at  $r = 10$  mm, it is interesting to see that the sample has been re-magnetised to 80% of  $J_c$ . However, the current density on the edge has decreased to zero. As the trough region travels at  $r = 20$  mm as in Fig. 2(g), the current density on the edge reverses direction to about 80% of  $J_c$  as shown in Fig. 2(h). Meanwhile, we have seen a clear increase of flux density in the centre of the sample. As the wave travels further into the sample as shown in Figs. 2(i) and 2(j), we can see that the current density between  $r = 10$  mm and 20 mm decreases, while the flux



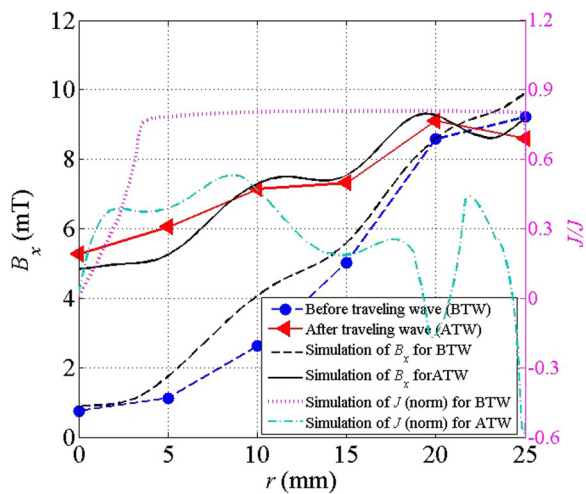


FIG. 3. The magnetic gradient measured 1.5 mm above the sample and calculated current density distribution before and after applying the traveling wave.

density in the centre increases further to 5.2 mT. Comparing the current density profiles in Figs. 2(h) and 2(j) with Figs. 2(d) and 2(f), we can also see that as the trough region travels into the superconductor, the central region has been gradually magnetised.

Fig. 2 only shows the first 6.83 s during the first cycle of the traveling wave. As shown in our previous publication, the increase of the flux density in the centre of the sample happens mostly in the first three cycles (predominantly the first period).<sup>4</sup> The following cycles do not change the magnetization very much. In Fig. 3, we show the final field profile after applying the traveling wave (over 12 periods). This result is compared with the field profile before the traveling wave was applied. The calculated current densities are also plotted in the figure. It is quite clear that, after applying the traveling wave, the magnetic gradient had been decreased drastically. Moreover, the simulation results show that, before applying the traveling wave, the current density is almost uniform across the sample (about 80% of  $J_c$ ). However, after applying the traveling wave for 12 cycles, the current density distribution inside the sample has become very complicated. In general, the value of current density has become much smaller than its critical current.

There are some arguments that the decrease in current density might also been caused by the cross field effect<sup>12</sup> or the flux shaking effect.<sup>17</sup> In our FEM model, we have tested the field in the centre of the gap where the superconducting sample is placed. The results shows that there is absolutely no cross field, i.e., the field parallel to the sample surface is zero. The applied field is always normal to the sample surface, so this cannot be caused by the cross field effect. Moreover, there are some arguments to say that the flux shaking in the direction normal to the sample surface might also cause such effect. However, as shown in our previous publication,<sup>4</sup> a standing wave normal to the sample surface does not “shake” the flux in the YBCO sample. As a matter of fact, it follows the Bean model prediction quite well.

In this experiment, we have shown that the magnetisation caused by the traveling wave is much more complicated than caused by a standing wave, i.e., it does not follow the constant current density assumption as suggested by the Bean model. The field inhomogeneity in space can lead to local variations of current density inside the type-II superconducting thin film, which is more likely to compromise the existing magnetic gradient as suggested by our experiment. This effect should be considered in the ac loss calculations especially for superconducting motors.

Also, we have shown that the traveling wave is more efficient in transporting the flux inside the YBCO sample. This interesting vortex dynamics phenomenon might suggest that the traveling wave can be used to magnetize type-II superconducting coils: in the case of a superconducting loop, such as superconducting coils, the traveling wave may help the vortices migrate from outside into the loop, which could gradually magnetize the superconducting coils as shown in Hoffman's<sup>6</sup> and Bai's<sup>5</sup> works. The mechanism of this flux pump shows complete distinction from the conventional type-I superconducting flux pump, in which the flux migrates with the help of normal spots.<sup>18</sup>

The authors would like to acknowledge Dr. D. Hasko and Mr. J. Grundy for their help and Ceraco Ceramic Coating GmbH, Germany for providing the YBCO sample.

<sup>1</sup>C. P. Bean, *Rev. Mod. Phys.* **36**(1P1), 31 (1964).

<sup>2</sup>W. J. Carr, *AC Loss and Macroscopic Theory of Superconductors* (Taylor & Francis, London, 2001), p. 13.

<sup>3</sup>E. H. Brandt, *Phys. Rev. B* **58**(10), 6506 (1998); **49**(13), 9024 (1994).

<sup>4</sup>W. Wang and T. A. Coombs, *J. Appl. Phys.* **113**(21), 213906 (2013).

<sup>5</sup>Z. Bai, G. Yan, C. Wu, S. Ding, and C. Chen, *Cryogenics* **50**(10), 688 (2010).

<sup>6</sup>C. Hoffmann, D. Pooke, and A. D. Caplin, *IEEE Trans. Appl. Supercond.* **21**(3), 1628 (2011).

<sup>7</sup>R. M. Walsh, R. Slade, D. Pooke, and C. Hoffman, *IEEE Trans. Appl. Supercond.* **24**(3), 4600805 (2013).

<sup>8</sup>W. Wang, M. Zhang, C. Hsu, and T. Coombs, *IEEE Trans. Appl. Supercond.* **22**(3), 5201304 (2012).

<sup>9</sup>W. Wang, R. Semerad, F. Spaven, M. Zhang, C. H. Hsu, Z. Zhong, Y. Chen, Z. Huang, and T. A. Coombs, *IEEE Trans. Appl. Supercond.* **23**(3), 8201104 (2013); W. Wang, M. Zhang, Z. Huang, Y. Zhai, Z. Zhong, F. Spaven, M. Baghdadi, and T. Coombs, *ibid.* **24**(3), 4600304 (2013).

<sup>10</sup>T. A. Coombs, O. Hadeler, M. Zhang, and K. Matsuda, *Supercond. Sci. Technol.* **25**(10), 104007 (2012); T. A. Coombs, Z. Hong, X. Zhu, and G. Krabbes, *ibid.* **21**(3), 034001 (2008).

<sup>11</sup>Y. D. Chung, I. Muta, T. Hoshino, T. Nakamura, and M. H. Shon, *Cryogenics* **44**(11), 839 (2004).

<sup>12</sup>P. Vanderbemden, Z. Hong, T. A. Coombs, S. Denis, M. Ausloos, J. Schwartz, I. B. Rutel, N. Hari Babu, D. A. Cardwell, and A. M. Campbell, *Phys. Rev. B* **75**(17), 174515 (2007).

<sup>13</sup>E. H. Brandt and G. P. Mikitik, *Phys. Rev. Lett.* **89**(2), 027002 (2002).

<sup>14</sup>Z. Hong, A. M. Campbell, and T. A. Coombs, *Supercond. Sci. Technol.* **19**(12), 1246 (2006).

<sup>15</sup>M. Zhang, J. Kvitkovic, J.-H. Kim, C. H. Kim, S. V. Pamidi, and T. A. Coombs, *Appl. Phys. Lett.* **101**(10), 102602 (2012).

<sup>16</sup>Y. Yeshurun, A. P. Malozemoff, and A. Shaulov, *Rev. Mod. Phys.* **68**(3), 911 (1996).

<sup>17</sup>M. Willemin, C. Rossel, J. Hofer, H. Keller, A. Erb, and E. Walker, *Phys. Rev. B* **58**(10), R5940 (1998).

<sup>18</sup>L. J. M. van de Klundert and H. H. J. ten Kate, *Cryogenics* **21**(4), 195 (1981).